

Simulating Non-linear Mode Coupling in Low Density Non-neutral Plasma using Computational
Methods

Physics 492R Capstone Project Report

Mitchell Clingo

5/25/18

Advisor: Dr. Grant Hart

© 2018, Mitchell Clingo

Abstract

Non-neutral plasma in a Malmberg-Penning trap has been shown computationally to exhibit nonlinear mode coupling between Trivelpiece-Gould modes. We used a computational model that shows similar mode coupling between the $n_z=1$ and $n_z=2$ modes. This occurs because of the nonlinear terms found in the momentum and the continuity equations. By driving both modes, we can get large enough magnitudes to see the coupling. If the magnitude of either mode is not large enough, coupling factors become insignificant. Also, a relation exists between the relative phase difference between modes and the direction of energy transfer in coupling.

Introduction

Hart, Spencer, and Peterson¹ have previously done work analyzing the nonlinear effects in waves in a nonneutral plasma, primarily using high densities in their analysis. This work was both done computationally and experimentally. Their model shows how these nonlinear effects are observed in high density plasma. This low-density study will support their findings, allowing better understanding of confined plasma behavior.

The momentum (Equation 1) and continuity (Equation 2) equations, shown below, each contain nonlinear terms, $(\mathbf{v}_e \cdot \nabla)\mathbf{v}_e$ and $\nabla \cdot (n_e \mathbf{v}_e)$, which are negligible at low oscillation magnitudes, but play a significant role in mode coupling when the oscillation magnitudes are big².

$$mn_e \left[\frac{\delta \mathbf{v}_e}{\delta t} + (\mathbf{v}_e \cdot \nabla)\mathbf{v}_e \right] + en_e \mathbf{E} = 0 \quad (1)$$

$$\frac{\delta n_e}{\delta t} + \nabla \cdot (n_e \mathbf{v}_e) = 0 \quad (2)$$

Assuming modes of the form

$$n_1 = n_{10} \sin(\omega_1 t) \sin(k_1 z)$$

$$n_2 = n_{20} \sin(\omega_2 t + \varphi) \cos(k_2 z)$$

the corresponding velocities are

$$v_1 = \frac{n_{10} \omega_1}{n_0 k_1} \cos(\omega_1 t) \cos(k_1 z)$$

$$v_2 = \frac{n_{20} \omega_2}{n_0 k_2} \cos(\omega_2 t + \varphi) \sin(k_2 z)$$

When applied to the continuity equation, the terms with the same spatial and temporal dependence as the n_1 and n_2 modes are

$$\frac{\delta n_{10}}{\delta t} = \frac{n_{10}n_{20}}{2n_0} \omega_1 \cos \varphi$$

$$\frac{\delta n_{20}}{\delta t} = -\frac{n_{10}^2}{2n_0} \omega_1 \cos \varphi$$

φ refers to the phase difference between the two modes, n_1 and n_2 . These differential equations demonstrate the non-linear coupling between the two lowest-order Trivelpiece-Gould modes, each containing terms from the other mode. In the coupling, one mode's large magnitude will cause an increase or decrease in magnitude of the other mode depending on the relative phase, acting as an alternating energy transfer between the two modes. This transfer alternates, both from the n_1 mode to the n_2 mode and from the n_2 mode to the n_1 mode, depending on the relative magnitudes and relative phase between the modes.

Because each mode has its own phase, calculating for φ , the relative phase difference between the two modes, is necessary. φ is used as a phase shift for the ω_2 frequency, if the phase in the ω_1 frequency is zero. Calculating for φ yields our reasoning for our calculation in Figure 3.

$$F(t) = \cos(\omega_1 t) + \cos(\omega_2 t + \varphi) = \cos(\omega_1 t + \varphi_1) + \cos(\omega_2 t + \varphi_2)$$

$$F(t) = \cos(\omega_1(t - t_0)) + \cos(\omega_2(t + t_0) + \varphi_2)$$

$$\varphi_1 = -\omega_1 t_0 \rightarrow t_0 = -\frac{\varphi_1}{\omega_1}$$

$$\varphi = \varphi_2 + \omega_2 t_0$$

$$\varphi = \varphi_2 - \frac{\omega_2}{\omega_1} \varphi_1$$

Because ω_2 is twice that of ω_1 when the modes are coupled, the equation can simplify to the following.

$$\varphi = \varphi_2 - 2\varphi_1$$

Through this simple equation, we can find the phase relationship between the two modes.

When the product of the low order mode term and the high order mode term are found in the continuity and momentum equations, we get the following.

$$2 \cos(\omega_1 t) \cos(\omega_2 t + \varphi) = \cos((\omega_2 + \omega_1)t + \varphi) + \cos((\omega_2 - \omega_1)t + \varphi)$$

This trig identity helps explain the mode coupling energy transfer from ω_1 to ω_2 and back, depending on the relative phase between the two modes. Because ω_2 is almost exactly twice the frequency as ω_1 , the difference term essentially becomes ω_1 , making the $n_z=1$ mode grow. The addition term does the opposite, making the ω_1 term shrink while the ω_2 term grows.

This explains the mode coupling caused by the nonlinear terms in the momentum and continuity equations.

Methods

In this computation, we ran a particle-in-cell code, designed to model the behavior of particles under electromagnetic influences using a fixed-mesh grid. In each time step, the code calculates the particles' motion equations and fields, and moves the particles in each time step accordingly. Our grid was structured in a cylindrical coordinate system, simulating the behavior of the plasma using previously published code³. The code takes in parameters for a Malmberg-Penning trap, including plasma properties, drive frequency and voltage, and time steps to run the simulation. The code then uses those parameters to act on a pre-calculated plasma equilibrium state, making the plasma fluctuate.

We have been studying electrostatic Trivelpiece-Gould modes in a nonneutral plasma. Our plasma is about 104 cm long and about 2 cm in radius. The plasma temperature is about 0.2 eV. The plasma is driven at the ends with alternating 5V potential differences, at the frequency to excite the $n_z=2$ mode. The plasma density was shifted by a given number of points from the equilibrium position to excite the $n_z=1$ mode. If the $n_z=1$ mode was too small, we did not observe any mode coupling.

We altered the plasma equilibrium state to impose a pre-existing $n_z=1$ mode by shifting all plasma particles several grid points to one side. Then, by driving the plasma at the ω_2 frequency, we provided an increase in magnitude of the ω_2 frequency to a magnitude where nonlinear effects were observed.

The data returned from the simulations was analyzed, providing the center of mass of the plasma and the root-mean-squared (RMS) length of the plasma. The center of mass shifts as the plasma moves side to side, characteristic of a half-wavelength mode, and the RMS length shifts as the length of the plasma grows and shrinks, characteristic of a full-wavelength mode. Thus, these two measurements correlate to their respective $n_z=1$ and $n_z=2$ modes. Because of the oscillating nature of the modes, we performed a least-squares fit to subsets of the center of mass and RMS length data of the plasma. Each subset was about 3000 data points – about 3-6 periods long, depending on the mode – providing enough points for an accurate least-squares fit, and a small enough section for decent resolution of the magnitude and frequency variations between subsets. We fit the data points to the equation $A \sin(\omega t + \varphi) + B$, fitting for the magnitude of the waves (A), the frequency of the waves (ω), the phase offset of the waves (φ), and the y-offset of the waves (B).

The returned fit variables allowed a relative plot of the magnitude, frequency, and phase of each mode from each subset of data. The magnitude plots are shown in Figures 2a and 3a. The frequency plots, scaled to the average ω_2 frequency, are shown in Figure 2b. The plot in Figure 3b shows relative phase values φ , adjusted to fit within $-\pi < \varphi < \pi$.

Results

There were two significant findings in this research. First, the nonlinear coupling between the modes is clear, and we can see the energy transfer between these modes. In Figure 1, the two modes from the same run are shown on an equal timescale, with negative time values being the time when the $n_z=2$ mode was driven. This run had enough magnitude in both modes to clearly show the mode coupling. This mode coupling is demonstrated by the magnitude shifts back and forth between the two modes. We can see a general plot of the comparative magnitudes of these modes in Figures 2a and 3a. It is significant to note that the coupling causes large shifts in energy, until at one time, most of the energy is held in either of the two modes, and the other mode has very little energy stored within. These energy peaks alternate between modes. In Figure 2b, we see how these modes link together in frequency, so that the frequency of $n_z=2$ is consistently twice that of the $n_z=1$ mode.

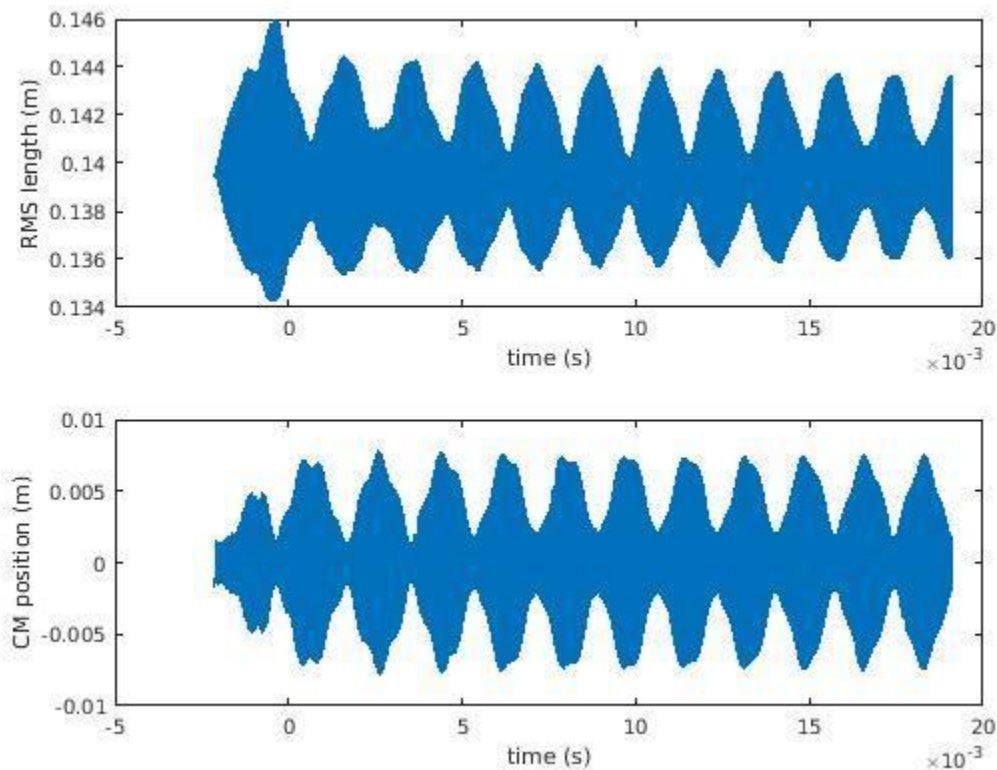


Figure 1: The fluctuating RMS length ($n_z=2$) and shifting center of mass ($n_z=1$) from one run. Time before $t=0$ indicates time where the plasma was being driven. Mode coupling can be seen, as one mode increases in magnitude, the other decreases, and vice versa.

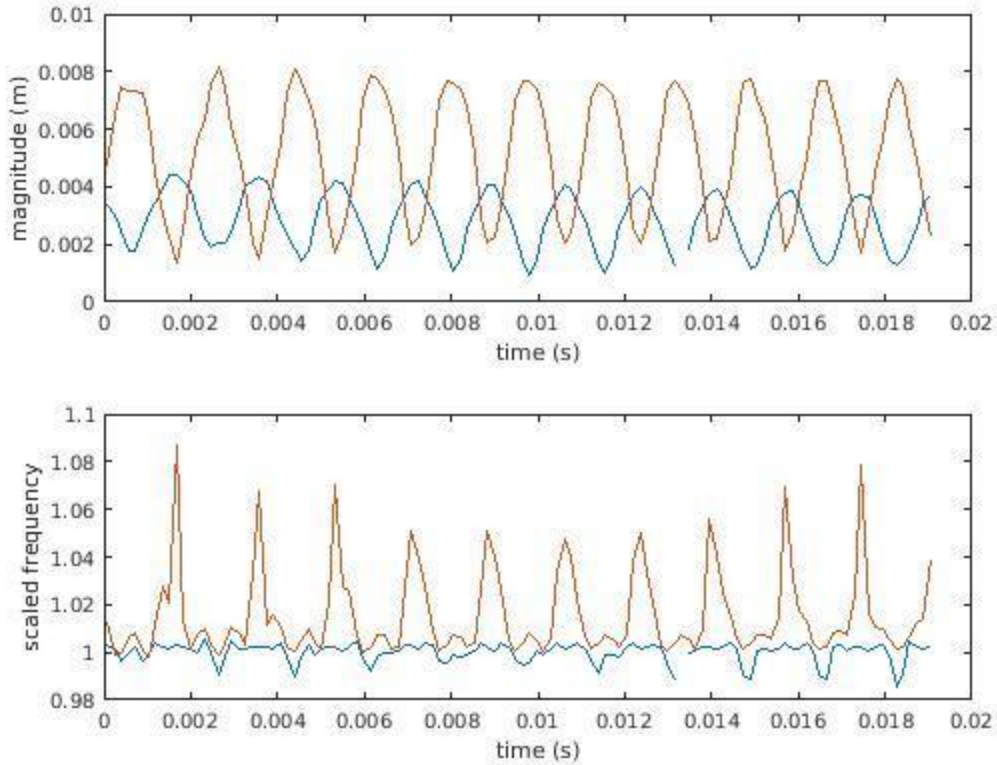


Figure 2: The orange lines pertain to the $n_z=1$ mode, and the blue lines to the $n_z=2$ mode. Figure 2a shows the relative magnitudes of the two modes, as calculated in the least-squares fit. Figure 2b shows a scaled frequency plot, where the blue line is equal to $\omega_2/\text{mean}(\omega_2)$ and the orange line is equal to $2\omega_1/\text{mean}(\omega_2)$. Note, the missing point in the plots is a point where the least-squares fit failed to fit properly.

We see in Figure 2 that the coupling is strong when the $n_z=1$ mode is large. This coupling causes the ω_1 frequency to be as close to $\omega_2/2$ as possible, within reasonable error. Yet, when the $n_z=1$ mode is small, the mode coupling is weaker, and we can see the departure from the mode frequency linkage. The points where the first mode departs from being half the frequency of the second mode reveals weak nonlinear mode coupling. It has yet to be determined why the ω_1 frequency increases to the value that it does at these low peaks in magnitude.

The second significant finding involves the relationship between phase and magnitude of the modes. When $-\pi/2 < \varphi < \pi/2$, the $n_z=1$ mode converts its energy to the $n_z=2$ mode. Points where this is true for φ are marked in Figure 3, and the points in the magnitude plots corresponding to those times for φ are also marked. Noticeably, when $\varphi < -\pi/2$ or $\varphi > \pi/2$ (φ is limited between $-\pi$ and π), the $n_z=2$ mode converts its energy to the $n_z=1$ mode.

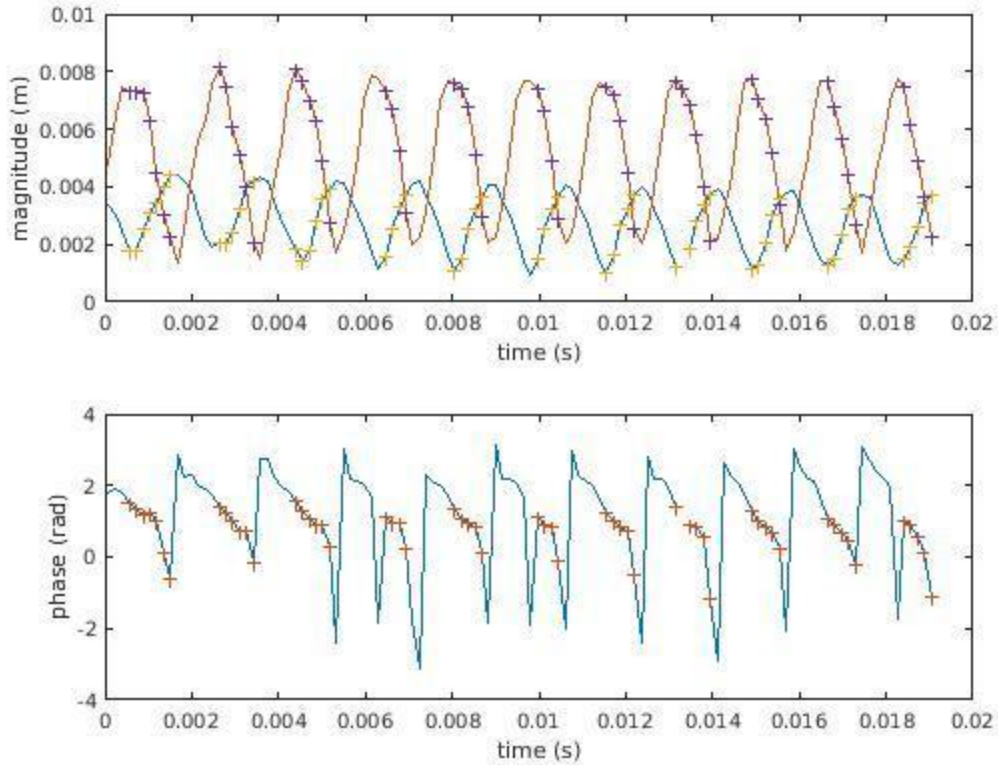


Figure 3a: The orange line pertains to the $n_z=1$ mode, and the blue line to the $n_z=2$ mode. Figure 3a shows the relative magnitudes of the two modes, the same as in Figure 2a. Points marked with a '+' are points at times where $-\pi/2 < \phi < \pi/2$. Figure 3b shows ϕ , calculated as $\phi_2 - 2\phi_1$. Points marked with a '+' are points at times where $-\pi/2 < \phi < \pi/2$. Note, the missing point in the plots is a point where the least-squares fit failed to fit properly.

Conclusion

Through these simulations, we see that the first two lowest-order Trivelpiece-Gould modes are strongly coupled when both modes have large magnitudes, as expected from the nonlinear terms in the momentum and continuity equations. Also, a correlation can be seen between the relative phase, ϕ , and the direction of energy transfer between modes. Further research can be done to better understand the departure frequency of the $n_z=1$ mode, when this mode becomes small. Also, higher-order modes can be studied to see how the energy transfer behaves differently with different ω_{n+1}/ω_n ratios.

References

- (1) Hart, Grant; Spencer, Ross; Peterson, Brian; Abstract: UP11.00008: Simulating the experimental detectability of axisymmetric Bernstein modes in a finite-length non-neutral plasma; 59th Annual Meeting of the APS Division of Plasma Physics, Volume 62, Number 12. <http://meetings.aps.org/link/BAPS.2017.DPP.UP11.8>

- (2) Chen, Francis F. Introduction to Plasma Physics and Controlled Fusion, 2nd ed. (Plenum Press, New York, 1983).
- (3) Hart, Grant; Spencer, Ross; (2013). Properties of axisymmetric Bernstein modes in an infinite-length non-neutral plasma. Physics of Plasmas, 20(10), 102101.

Acknowledgements

I would like to express gratitude towards Dr. Grant Hart for his invaluable support, advice, and assistance with the concepts and computational methods. I would also like to acknowledge Dr. Brian Peterson for both guidance in the project and for sharing significant computing power and data storage for the project.